

# Gas turbine engine condition monitoring wirelessly by vibration energy harvesting

Dr. Daisy Rani Alli<sup>1</sup>, A.S.R Kaushik<sup>2</sup>

1. Asst Professor, Instrument Technology, Andhra University, Visakhapatnam, Andhra Pradesh, India, 530017. Email: [a\\_daisyrani@yahoo.com](mailto:a_daisyrani@yahoo.com)
2. Instrument Technology, Andhra University, Visakhapatnam, Andhra Pradesh, India, 530017. Email: [kaushikasr@gmail.com](mailto:kaushikasr@gmail.com)

***Abstract-*** *The condition monitoring of the Gas Turbines is carried about by a commercially available wireless mote module called the TelosB Mote which has a sensor suite. Vibration energy is harvested using a Piezoelectric polymer sensor loaded with mass. A power management module is designed. The vibration sensor and the power management module are used to satisfy the power requirements of the TelosB Mote. The sensor performance is analysed and found to have a baseline sensitivity of 1.1 V/g and produces 0.207 mV for 75 Hz. The power management module is fabricated and tested. The module comprises of AC-DC rectification, storage of energy and switching the power from sensor to the application circuit. The power requirement is optimized as the sensor data is obtained at discontinuous intervals. The light surrounding the engine is monitored remotely on PC by an on-board sensor of the mote. Different parameters determining engines efficiency can be monitored by integrating the respective sensors to the mote.*

***Key Words:*** *TelosB mote, vibration, piezoelectric polymer sensor.*

## I. INTRODUCTION

Gas Turbines, due to their better efficiency have a wide applications in power generation, transportation, and other industries. The efficiency of the gas turbine is influenced by many parameters such as ambient air temperature and pressure, elevation, relative humidity, compressor pressure ratio, blade tip clearance, type of fuel used, etc. Hence the necessity to monitor the condition of the engine arises. Wired sensor networks with miles of cabling is expensive to install and maintain. Hence, a network of autonomous vibration powered, wireless sensors provide a “fit and forget” solution to the problem of data collection.

The major components in any wireless sensor networks are its power supply. The use of battery limits the use of many wireless sensor nodes as the batteries wear out when used continuously. It also limits the deployment of sensors at a larger scale, owing to the power consumption. Regular replacement of batteries for larger networks is also impractical. Hence utilizing the ambient energy surrounding the engine, the deployment of the wireless sensor networks for monitoring large structures such as engines, is feasible. The vibration energy surrounding the engine is harvested

using a piezoelectric polymer device loaded with mass, owing to its large power densities and able to sustain larger mechanical strains and oscillations [1]. Piezoelectric materials were used previously in shoes and other RF applications [2]. The mass is used to increase the sensitivity. It is integrated to a TelosB mote module which determines the condition of the engine by wirelessly monitoring the condition of engine at a distant place.

## II. DESIGN

### *Self Powered sensor node architecture*

The standard unit of any wireless sensor system is the wireless sensor node. The basic functionality of it is to collect the data and transmit it to the base station. Here, we use two TelosB motes, such that one of them is powered by the harvested vibration energy, which is to be placed on the engine, and the other is connected to the PC which acts as a base station (Fig. 1). The nodes are programmed in such a way that, the self powered sensor node transmits the value of the sensors on its sensor suite and the other node is connected to the PC which receives the values and displays them on the monitor by which the condition of the engine is monitored wirelessly.

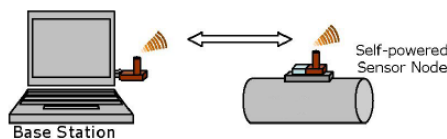


Figure 1. Wireless Sensor Network Schematics

The basic components of a sensor node that fulfils the requirement of general sensor

monitoring applications are as shown in Figure 2.

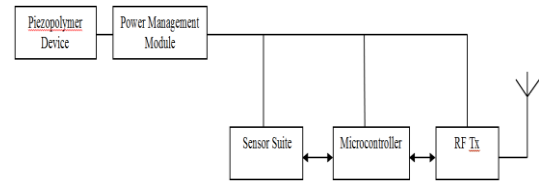


Figure 2. Schematics Of Self Powered Sensor Node

Many Ultra-Low power electronic components such as Sensirion SHT11 sensor, Photodiodes such as S1087 and S1087-01 to sense photosynthetically active radiation and entire visible spectrums, TI MSP430 microcontroller and Chipcon 2420 transceiver are used to get the desired functionality above. A commercially available TelosB mote which integrates all of these components is henced used for our purpose.

Power management module serves three basic functions:

- Rectification Of sensor output to DC voltage.
- Storage of the rectified output.
- Active switching between the power source and the application circuit.

### *1. AC-DC rectifier*

Generally, the Piezoelectric device producing the AC signal is rectified using either a bridge rectifier or an voltage doubler circuit. It was previously tested using a full wave rectifier [3]. The former use is

constrained by the four voltage drops across the diodes. Moreover, in the full bridge configuration, the rectified voltage ( $V_{rec}$ ) under no-load condition is ideally equal to the peak open-circuit voltage at the piezoelectric terminals ( $V_{oc}$ ) whereas in the voltage doubler, the no-load voltage is twice this voltage ( $2V_{oc}$ ). Ottman et al. analytically showed that for the full bridge configuration, the maximum power extracted from a piezoelectric device occurs when the rectified voltage is maintained at one-half of the no-load voltage (i.e.  $V_{rec}=V_{oc}/2$ ). By using similar analysis, one can show that for the voltage doubler configuration, the maximum power extraction occurs when the rectified voltage is also one-half of no-load voltage i.e.  $V_{rec}=2V_{oc}/2=V_{oc}$ . The circuit diagram for it is as shown in figure 3.

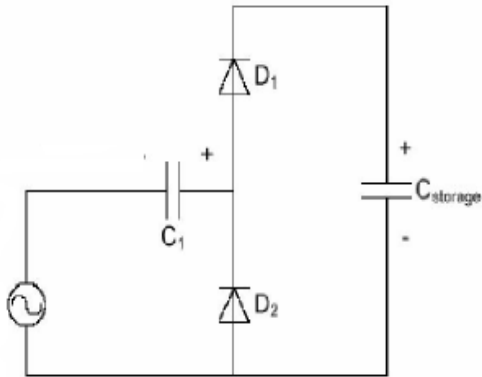


Figure 3. Voltage Doubler Rectifier

Two diodes  $D_1$  and  $D_2$  are used in the configuration which are STMicroelectronics IN5711 diodes.  $C_1$  serves as an intermediary energy storage capacitor.  $C_{storage}$  is the storage capacitor and relatively large compared to  $C_1$ . During the negative half cycle of sinusoidal input,  $D_2$  is forward biased, connecting the positive terminal of

$C_1$  to ground.  $C_1$  charges upto a maximum negative voltage (or positive according to polarities indicated in figure). This voltage is dependent on the frequency and the amplitude of vibrations. During the positive cycle,  $D_2$  is reverse biased.  $D_1$  becomes forward biased, connecting the  $C_1$  to charging capacitor  $C_{storage}$ . This power flow scheme is repeated for each cycle.

## 2. Active Switching By Voltage Monitoring Module

The vibrations in the engine are not sustained ones. Moreover, a single piezoelectric polymer device cannot provide sufficient energy to power Telos continuously. Most of the condition monitoring applications do not require continuous streams of sensor data as well. Hence the power management module is designed in such a way that TelosB mote is powered at discontinuous intervals. Energy is first transferred to a storage capacitor ( $C_{storage}$ ) during the charging mode. Once the capacitor as stored sufficient energy, the module will switch the power from the storage capacitor to the TelosB Mote in the active mode.

The  $C_{storage}$  is connected to the Piezoelectric device and charged upto  $V_{high}$  during the charging mode. Once, the  $V_{C_{storage}}$  reaches  $V_{high}$ , a single pole double throw (SPDT) switch connects the TelosB mote. As Telos consumes energy,  $V_{C_{storage}}$  drops to  $V_{low}$ , the active mode ends and the charging mode begins. Voltage is monitored across  $C_{storage}$  with the help Maxim MAX9118 comparator and SPDT switch Intersil ISL84714. The threshold voltages are set using  $R_1$ ,  $R_2$ ,  $R_3$  and  $R_4$  of  $1M\Omega$ ,  $1.1M\Omega$ ,

1.8M $\Omega$  and 1M $\Omega$ .  $V_{high}$  is set to 3V and  $V_{low}$  is set to 2.2V, well between their threshold limits. Both the comparator and the switch are powered by  $C_{storage}$ . By this way, the energy utilization efficiency is increased and the mote is powered efficiently.

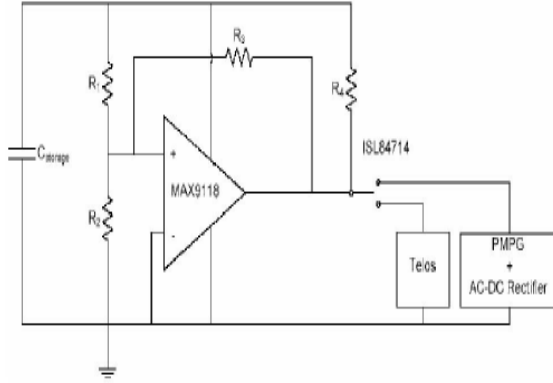


Figure 4. Schematics Of Voltage Monitoring Module

### III. POWER MANAGEMENT MODULE AND FABRICATION

#### A. Power Management Module

The voltage doubler rectifier and the voltage monitoring module as explained above, are integrated together to power the TelosB Mote module. The circuit schematic with the component values, for which the PCB is fabricated, is shown below.

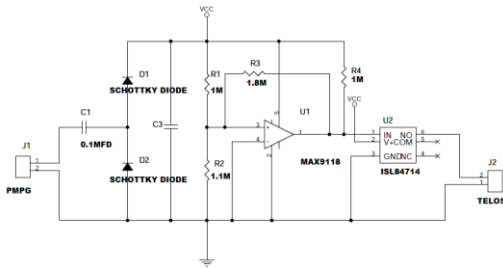


Figure 5. Circuit Diagram Used For Vibration Energy Harvesting

As shown in the figure 5, PMPG is the piezoelectric micro power generator (which is Minisense 100 sensor). STMicroelectronics 1N5711 diodes ( $D_1$  and  $D_2$ ) are used here for rectification.  $C_1$  serves as intermediary energy storage element between PMPG and the energy storage capacitor ( $C_3$ ).  $C_1$  is a 0.1 $\mu$ F ceramic capacitor and for  $C_3$ , two values, 1mF and 2.2mF electrolytic capacitors are used with two separate PCB boards. The voltage across the storage capacitor is monitored using a SPDT switch, Intersil ISL84714, and the Maxim MAX9118 comparator. The threshold limits of the storage capacitor are fixed with the resistor values. The resistance values shown are in ohms. Both the comparator and the switch are low power consumption components and are powered by  $C_3$ . The TelosB Mote is connected at the output of the switch.

#### B. Special Requirements

##### 1. Low Powered Analog Switch

The harvested power from the vibration sensor is less. The conventional analog SPDT switches are powered from approximately 4.5V and have high ON resistances. The rectified and doubled output will not satisfy the power requirement of these switches. Hence, low voltage, ultra low ON resistance which operates from single 1.65V to 3.6V supply is used. These switches are SMD components and typical  $r_{on}$  values are in and around 0.6 $\Omega$  depending upon the switch supply. The switching action of the switch is even faster, having  $t_{ON}$  of 7.5ns and  $t_{OFF}$  of 2.9ns for 2.7V supply.

##### 2. Nano power Comparators

One more constraint is the typical low current output of the sensor with high voltage output. It does not allow the normal comparators to be used which have power

requirements that cannot be met. Hence, a 1.6V, nanopower comparator having ultra low supply current of 600nA with open drain outputs is used in our experiment.

### C. PCB Design And Fabrication

The PCB board fabrication consists of a Through Hole part and an SMD part. The PMPG sensor (Minisense 100) is connected to the PCB with a male female connector and wires extending out from the PCB, so that the PCB does not get disturbed while the sensor is placed on the vibration source.

The through hole part of the PCB is till the storage capacitor ( $C_3$ ) i.e. the rectifier portion of the circuit containing ceramic and electrolytic capacitors and Schottky diodes. These are followed by resistors  $R_1$ ,  $R_2$ ,  $R_3$  and  $R_4$  which are SMD resistors.  $R_1$  and  $R_4$  are  $1M\Omega$  (0805) and  $R_2$  is  $1.1M\Omega$  (0402) and  $R_3$  is  $1.8M\Omega$  (0805). The comparator Maxim MAX9118 is of SMD followed by a SPDT switch Intersil ISL84714 of SMD. Till here the PCB is SMD configured. The output of the switch would be connected to TelosB module, hence wires are extended through a connector so as to connect the module.

The checkplot of the PCB is as shown in the figure 6. The PCB is fabricated on both sides. The top layer consists of the through hole part of the PCB, and the bottom layer consists of the SMD part of the PCB along with the interconnections path.

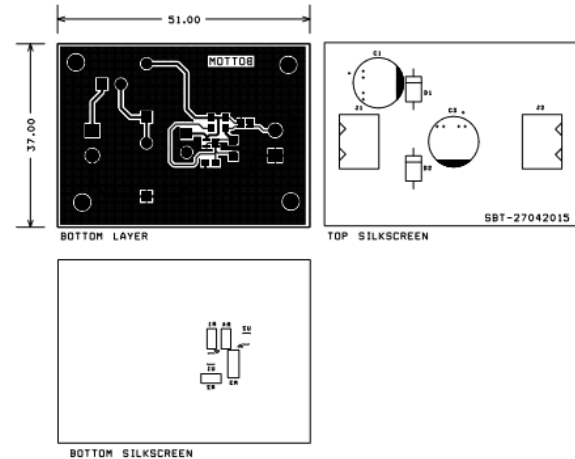


Figure 6. Checkplot of The Fabricated PCB

The top and the bottom view of the designed PCB before fabrication is as shown in figure 7.

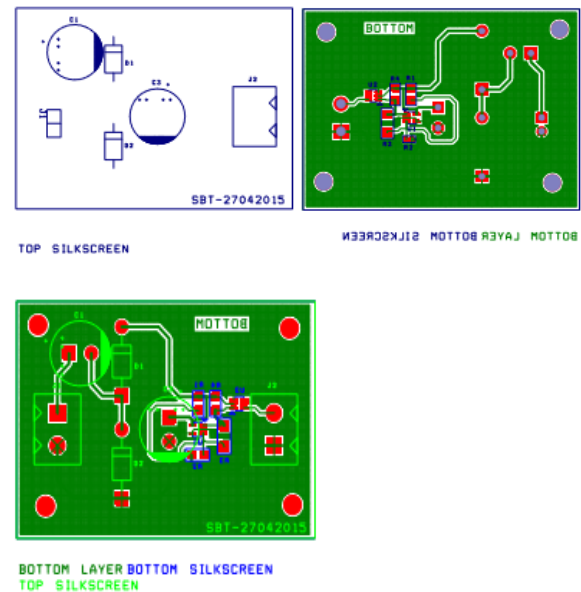


Figure 7. Top And Bottom View Of PCB Design

The dimensions of the PCB could be further reduced by a large factor. In order to test the PCB, and to hold it properly for feasibility, the dimensions are not being constrained. The fabricated PCB which is used for the experiment is as shown below.

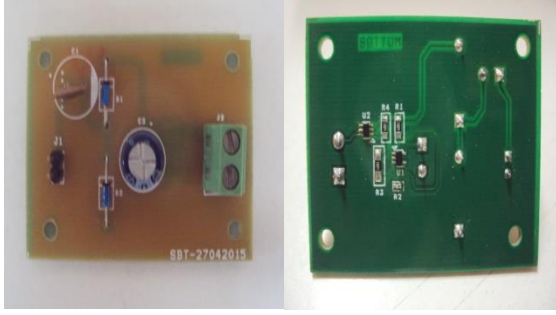


Figure 7. Top And Bottom View Of Fabricated PCB

The storage capacitance values were determined from the simulation of the circuit. The load (TelosB Mote) was considered to be  $1k\Omega$  resistor connected across the output terminals. Lower than  $1mF$  capacitance values resulted in providing insufficient energy to the TelosB mote with charging and discharging times being very less.

#### IV. RESULTS AND DISCUSSIONS

The performance of the vibration sensor was analysed for its power output. The sensor was terminated with a resistive load. The sensor was mounted on a vibrometer. The vibrometer is actuated by producing a sine wave from a signal generator, using the waveform as the input to a power amplifier and connecting the output of the power amplifier to the input of the vibrometer. The magnitude and frequency of the source waveform, and the gain of the power amplifier all affect the acceleration generated by the vibrometer. The magnitude of the source waveform was kept constant at 1 volt rms. Only the frequency and gain on the power amplifier were used to produce the desired vibrations. The sensor was allowed to operate with baseline sensitivity. The frequency and gain of the power amplifier were used to produce the desired vibrations. The input to the vibrometer was set to the natural frequency

of the sensor i.e. 75Hz. The power and the voltage output versus load resistance is as shown below.

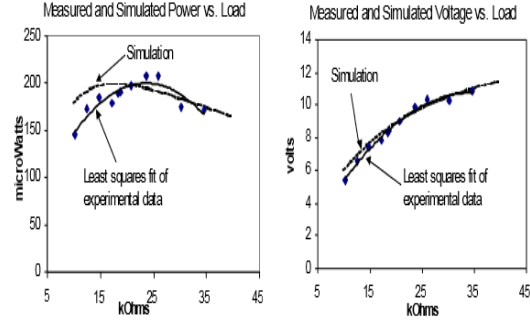


Figure 8. Sensor Power And Voltage Vs Load Waveforms

At resonance, i.e when the natural frequency of the sensor matches the frequency of the vibrometer, the maximal power output is obtained. The measured output power versus the drive frequency is given below.

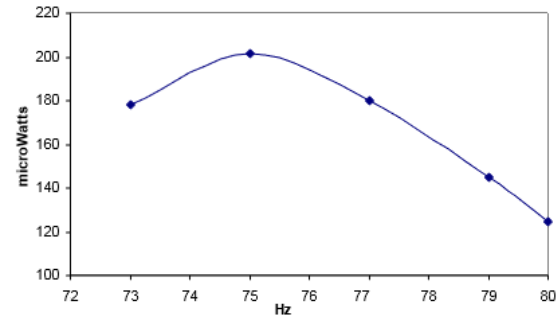


Figure 9. Output Power Vs Natural Frequency

A sinusoidal voltage source supposedly provided by the Vibration sensor is obtained using a function generator. Digital oscilloscope is used for measuring the voltage across the capacitor. The voltage at the output of the switch, which is used to power the mote (TPR2420), is measured using a multimeter. When the mote is powered, it is programmed such that the sensor suite transmits its sensor values (light intensity), which is received by another mote



(TPR2400) which is connected to a PC at base station. This node is programmed in such a manner that it receives the transmitted ADC values of the sensors on the mote. The values are displayed on the screen with the help of a Java program. It clearly shows the variation around the light sensor on its screen. The screenshot of the sensor values displayed is as shown below.

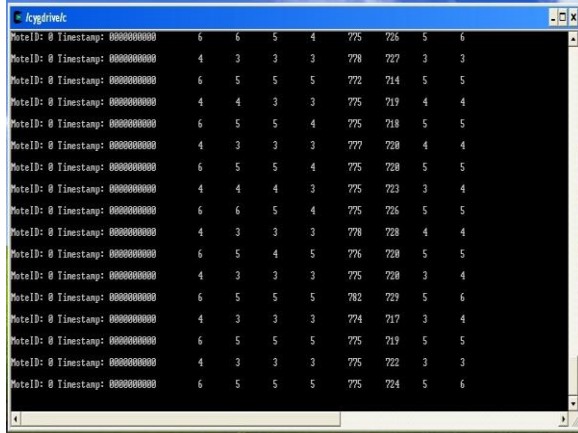


Figure 10. Screenshot Of Sensor Values

When the mobile node is placed on the engine, we can observe the variations in the amount of light surrounding the node effectively at the base station. The gas turbine engines efficiency is influenced by many parameters such as ambient air temperature and pressure, elevation, relative humidity, compressor pressure ratio, blade tip clearance, type of fuel used, etc. By integrating the mobile node with the sensor boards as per the parameters of the engine that need to be monitored, and following this harvesting procedure, the condition of the engine can be monitored effectively and efficiently.

## V. CONCLUSION

In order to monitor the various parameters of the gas turbine engine which

affects the performance of the engine, using the available ambient vibration energy surrounding the engine, a system architecture is designed. A new power management module is designed which satisfies the sensor nodes power requirement. A Piezoelectric polymer sensor loaded with mass (Minisense 100) is used for Vibration to electricity conversion. Polymer is used based on its larger power outputs coupled with the ability to withstand larger strains and the mass is used to increase its sensitivity. The output of the sensor is studied by placing it on the vibrometer and the power output after clamp losses was calculated to be  $207\mu\text{W}$  at  $75\text{Hz}$ . The power management module was developed to provide AC-DC rectification, energy storage and active switching between the sensor and the application node. The corresponding PCB was designed, fabricated and tested. The mote was powered by the harvester PCB and the amount of light surrounding the node was observed wirelessly from a distant place on the PC screen.

## REFERENCES

- [1] **S. Roundy, P. K. Wright, and J. Rabaey**, "A study of low level vibrations as a power source for wireless sensor nodes," *Computer Communications*, vol. 26, no. 11, pp. 1131-1144, 2003.
- [2] **J. A. Paradiso and T. Starner**, "Energy scavenging for mobile and wireless electronics," *IEEE Pervasive Computing*, vol. 4, no. 1, pp. 18-27, February 2005.
- [3] **Y. B. Jeon, R. Sood, J. H. Jeong and S.G. Kim**, "Piezoelectric Micro Power Generator for Energy Harvesting," *Sensors and Actuators A: Physical*, 122, No. 1, P16, 2005
- [4] **G. K. Ottman, H. F. Hofmann, A. C. Bhatt, and G. A. Lesieutre**,

"Adaptive piezoelectric energy harvesting circuit for wireless remote power supply," IEEE Transaction on Power Electronics, vol. 17, no. 4, pp. 669-676, 2002.

- [5] **A. S. Weddell, G.V. Merrett, S. Barrow, B.M. Al-Hashimi,** "VIBRATION-POWERED SENSING SYSTEM FOR ENGINE CONDITION MONITORING," IEEE paper, Electronics and Computer Science, University of Southampton, Southampton, SO17 1BJ, UK
- [6] **S. R. Anton and H. A. Sodano,** "a review of power harvesting using piezoelectric materials (2003–2006)," Smart Mater. Struct., vol. 16, no. 3, pp. r1–r21, 2007.
- [7] **Sabrie Soloman, Ph.D., Sc.D., MBA,** "Sensors Handbook", Second edition, Copyright © 2010, 1999 by The McGraw-Hill Companies, Inc.
- [8] **R. Amirtharajah and A. P. Chandrakasan,** "Self-Powered Signal Processing Using Vibration-Based Power Generation," IEEE J. Solid-State Circuits, 33 (1998) 687-695.
- [9] **S. Meninger, J. O. Mur-Miranda, R. Amirtharajah, A. P. Chandrakasan, and J. H. Lang,** "Vibration-to-Electric Energy Conversion," IEEE Trans. VLSI Syst., 9 (2001) 64-76.